The use of an improved technique to reduce the variability of output voltage in real-time Fibre Bragg Grating based monitoring system

The use of an improved technique to reduce the variability of output voltage in real-time Fibre Bragg Grating based monitoring system

E Vorathin[1*], Z M Hafizi[1], S A Che Ghani[2], K S Lim[3], A M Aizzuddin[1]

[1]Advanced Structural Integrity and Vibration Research (ASIVR), Faculty of Mechanical Engineering, University Malaysia Pahang (UMP), Pekan 26600 Pahang, Malaysia
[2]Human Engineering Group (HEG), Faculty of Mechanical Engineering, University Malaysia Pahang (UMP), Pekan 26600 Pahang, Malaysia
[3]Photonics Research Centre, Faculty of Science, University of Malaya, 50603 Kuala Lumpur, Malaysia

*Corresponding author: vora.91.11@hotmail.com

Abstract. Fibre Bragg Grating (FBG) sensors have been widely utilized in the structural health monitoring (SHM) of structures. However, one of the main challenges of FBGs is the existence of inconsistency in output voltage during wavelength intensity demodulation utilizing photodetector (PD) to convert the light signal into digital voltage readings. Thus, the designation of this experimental work is to develop a robust FBG real-time monitoring system with the benefit of MATLAB graphical user interface (GUI) and voltage normalization algorithm to scale down the voltage inconsistency. Low-cost edge filter interrogation system has been practiced in the experimentation and splitter optical component is make use to reduce the intensity of the high power light source that leads to the formation of noise due to unwanted reflected wavelengths. The results revealed that with the advancement of the proposed monitoring system, the sensitivity of the FBG has been increased from 2.4 mV/N to 3.8 mV/N across the range of 50 N. The redundancy in output voltage variation data points has been reduced from 26 data/minute to 17 data/minute. The accuracy of the FBG in detecting the load induced falls in the acceptable range of total average error which is 1.38 %.

1. Introduction

It is well apprehended that FBG sensors are far more superior in providing closer look upon defects compared to conventional Non-destructive testing (NDT) inspections. Most of the conventional NDT inspections are limited by the bulky size of the whole system making it impossible to be integrated with the structure as a whole. Furthermore, these inspections provide an off-line monitoring on the structures. Thus, specialized characteristics such as small physical size, immune to electromagnetic interference, light weight, relative signal stability and wavelength multiplexity [1-4] have turned researchers to make use of the FBGs in SHM of structures, especially in composite materials. However, much endeavour is still needed to bring the FBGs real-time monitoring system to a fully mature readiness level. One of the main challenges in converting the wavelength intensity demodulation utilizing PD is the existence of inconsistency in output voltage readings that could precede in error of desired readings and difficulty in value calibration. This complication has been

encountered by the authors of this paper as well as other researchers [5-7] who make use of the photodetector to alter the intensity demodulation to digital voltage readings. For instance, work by Allwood et al [6] has shown a significant variation of the voltage output which leads to errors in the measurement as shown in figure 1. High power from the light source is one of the reasons which outcome in a high intensity of the reflected wavelength in which unwanted wavelengths will present in the spectrum that could lead to wrong mismatching condition and affect the output voltage consistency. Implementation of voltage normalization algorithm will be the proposed problem-solver to reduce the voltage inconsistency.

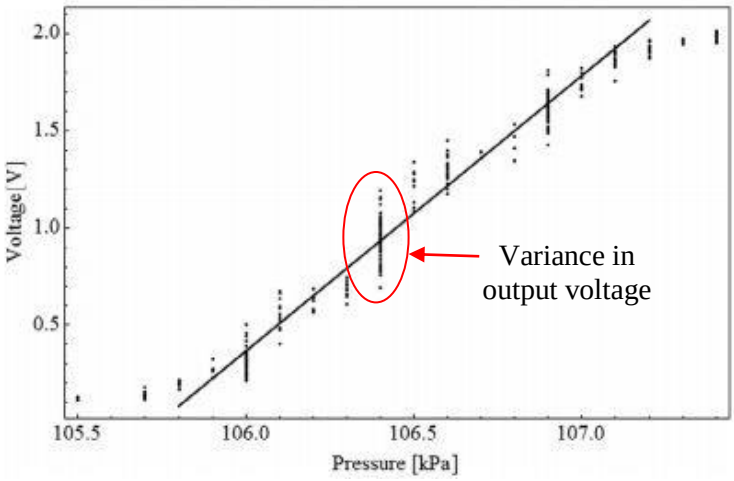

Figure 1. Variance in output voltage when photodetector was utilized for intensity to voltage conversion [6].

Normalization is a statistical analysis to scale down the redundancies of data in a database in which it is a technique of designing and redesigning a database [8]. Researches predominantly in social science [9-12] implement normalization in data analysis to reduce the variability of the desired output. Researchers in the field of FBGs [13, 14] have also employed this mathematical algorithm in normalized out the optical power or intensity values, however, the utilization of expensive signals precision devices such as optical interrogation unit and logging of data for post-processing are still the gap to be amended. Thus in this study, several configurations of interrogation system will be experimentally performed to demonstrate the root of the voltage inconsistency and at the end, a solution will be proposed.

2. Fibre Bragg Grating (FBG) sensor instrumentation and working principle

FBG is an optical fibre with laser inscribed in the core region known as Bragg grating. The grating reflects the wavelength as shown in figure 2 of the emitted light known as Bragg wavelength (λ_B) in which concerning with the grating period (Λ_o) formulate as [15]:

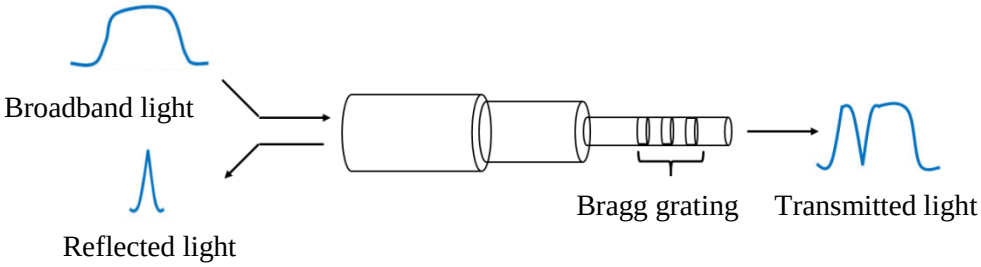

Figure 2. The working principle of FBG sensor.

$$\boldsymbol{\lambda_B = 2\eta_o\Lambda_o/\kappa} \quad (1)$$

where κ is the gratings order and $\boldsymbol{\eta_o}$ is the initial refractive index before subjected to strain. The Bragg wavelength also can be defined in term of refractive index of the grating ($\boldsymbol{\eta_{eff}}$) as:

$$\boldsymbol{\lambda_B = 2\eta_{eff}\Lambda_o} \tag{2}$$

Bragg wavelength shifts also can be modulated due to change of temperature, $\boldsymbol{\Delta T}$, and strain, $\boldsymbol{\varepsilon}$ can be denoted as [16, 17]:

$$\frac{\boldsymbol{\Delta\lambda}}{\boldsymbol{\lambda_B}} = (\hat{a} + \boldsymbol{\xi})\boldsymbol{\Delta T} + (\mathbf{1} - \boldsymbol{p_e})\boldsymbol{\varepsilon} \tag{3}$$

where $\boldsymbol{\Delta\lambda}$ is the change in wavelength, â is the thermal expansion, $\boldsymbol{\xi}$ is thermo-optic coefficient and $\boldsymbol{p_e}$ is the effective photo-elastic constant of the fibre. However, for an isothermal condition the change of temperature can be neglected which simplified the expression as [17]:

$$\frac{\boldsymbol{\Delta\lambda}}{\boldsymbol{\lambda_B}} = (\mathbf{1} - \boldsymbol{p_e})\boldsymbol{\varepsilon} \tag{4}$$

2.1. Experimental procedure and results

40 cm (length) x 40 cm (width) x 0.8 cm (thickness) of ten layers woven fibreglass composite plate was fabricated by the method of hand lay-up and cured by applying glycidyl (GL) epoxy and hardener as resin. A single 1544 nm FBG sensor with 99.9 % reflectivity was embedded at the centre between the ninth and tenth layers of the composites plate. The composite plate was clamped fixed at four edges and a weight support stand was positioned at the centre of the plate for equivalent and constant load distribution. The set-up was shown in figure 3a below. A 10 N and two pieces of 20 N known loads as in figure 3b were induced repeatedly on the composite plate starting from 0 N to 50 N with the increment of every 10 N. The experimental set-up undergoes three configurations and manipulation in interrogation system as detailed in figure 4.

Three different configurations of optical components namely optical circulator (15-PICIR- 3-SCL-1) - SET A, 50:50 intensity ratio optical coupler (CS-5250-S115-03) - SET B, and 1:8 intensity ratio optical splitter (OFC-CP1xN-034C) - SET C have been experimentally tested to determine the effect of high power ASE broadband light source on the reflected sensing FBG wavelength. Bayspec (FBGA-F-1525-1565-FP) optical spectrum analyzer (OSA) was used to view reflected spectrum.

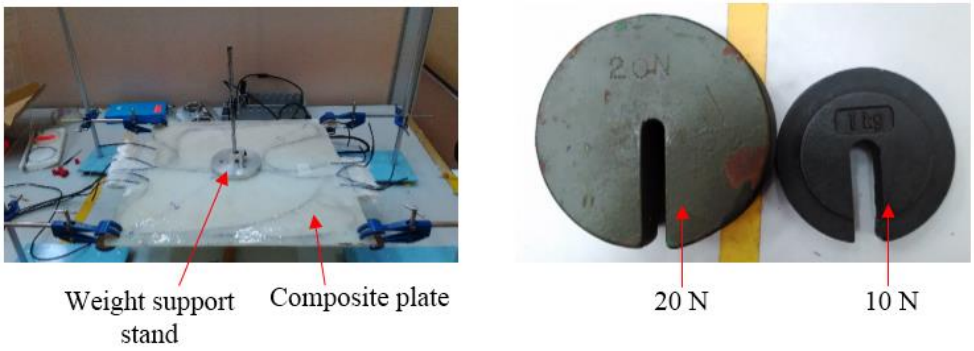

Figure 3. Experimental set-up: (a) Fixture of the specimen, (b) Loads used to induce on the plate.

Figure 5 shows the recorded and analyzed reflected wavelengths of the sensing FBG when no load induced from three different optical components namely SET A, SET B, SET C and also the overlaid graphs of the three components. Reflected wavelength for SET A shows the most severe wavelength distortions in which four unwanted wavelengths are present as shown in figure 5(a). Existent of peak splitting is also present in the spectrum and SET A shows the highest intensity recorded. 10.78% of intensity was reduced when SET B was adopted and the unwanted wavelengths were reduced to two as shown figure 5(b). SET C shows the most intensity reduction in which 66.47% of intensity has been reduced as shown in figure 5(c) compared to SET A and an ideal single Bragg wavelength was

obtained. From the overlay of all the reflected spectrum as shown in figure 5(d), clearly shows that different utilization of optical components result in different power intensity.

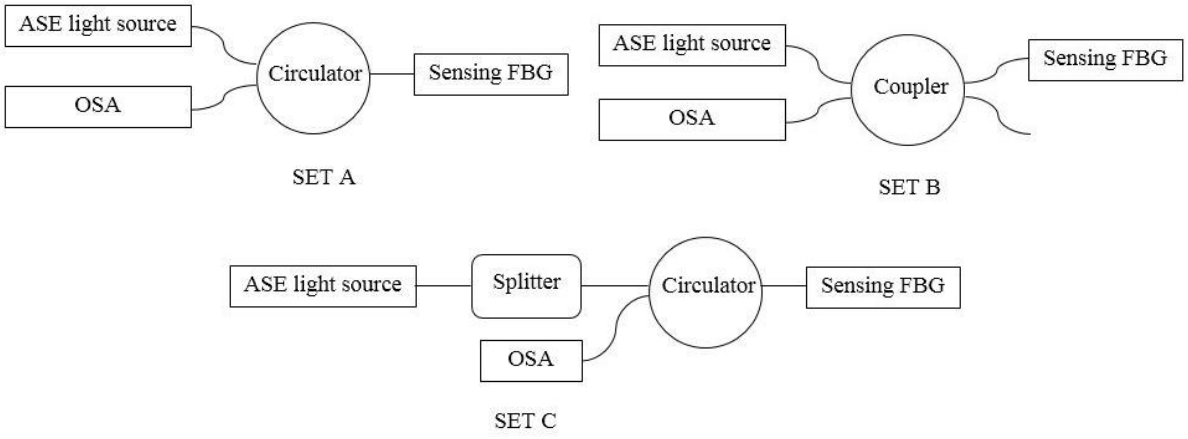

Figure 4. Configurations of the experimental set-up interrogation system.

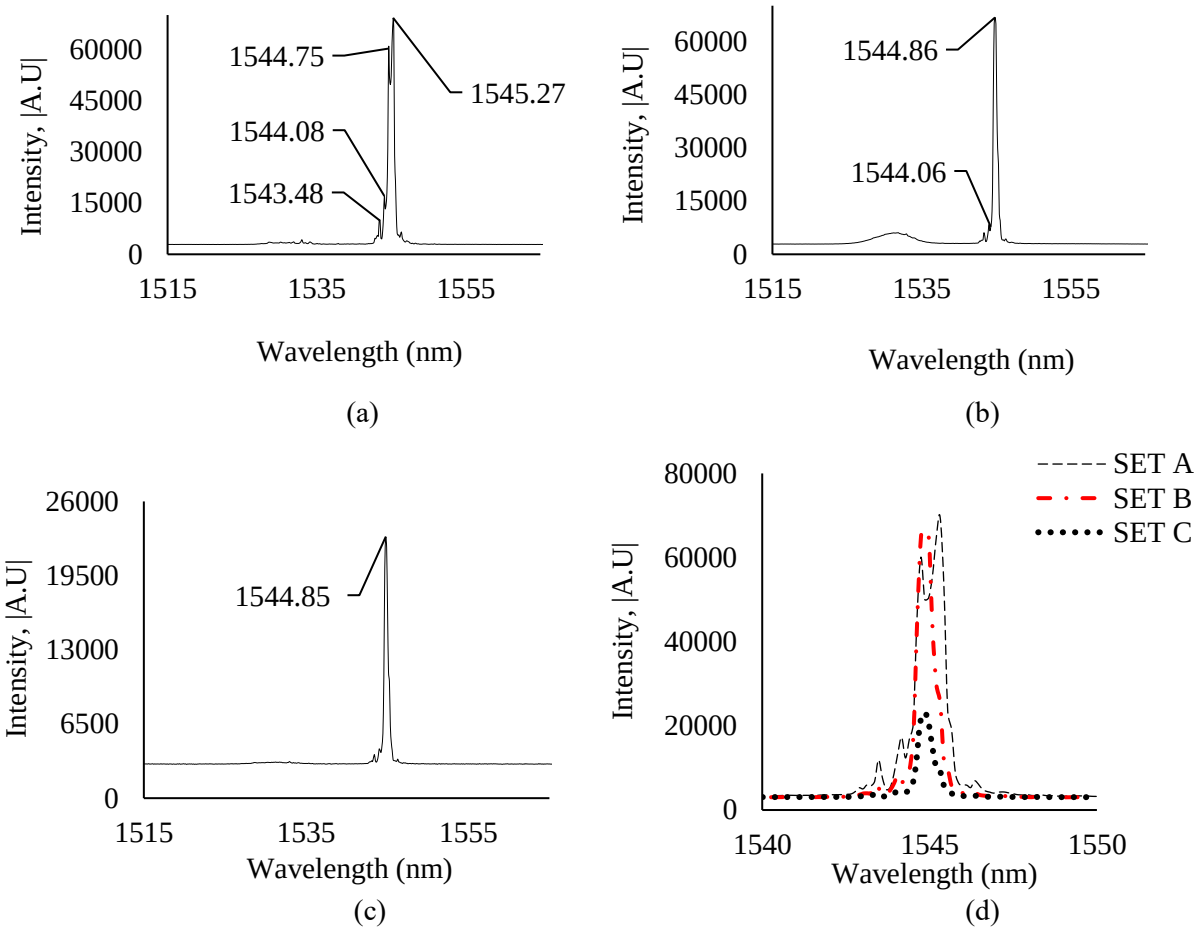

Figure 5. Reflected wavelengths of the sensing FBG from the three optical components which are: (a) SET A, (b) SET B, (c) SET C and (d) overlaid of the three.

3. Theoretical and experimental of edge filter detection due to static strain

Interrogation system is the working system used to illuminate the FBG sensors. There are two types of interrogation system namely power detection and edge filter detection [18]. In general, power detection interrogation benefits in dynamic strain detection due to the use of laser types light sources

such as linear edge source [19] and narrow bandwidth source [20]. Edge filter detection is the most economical and simplest among the interrogation system [21]. Edge filter detection utilized the use of broadband light source and employed a reference FBG to mismatch with the sensing FBG. Edge filter detection interrogation system has been reported earlier than the year 2000s, however, direct output voltage without normalization is being measured utilizing photodetector making this low-cost interrogation system non-stable due to the fluctuation of output voltages.

A PD is commonly practiced to read the demodulation shift of the reflected intensity into an analog voltage signal. Figure 6 below shows the working principle of the photodetector. The wavelength shift of the sensing FBG as labelled A will result in intensity variation when sensing FBG slide across the slope of the reference FBG as labelled B. As a sequel, the photodetector will transform the intensity variation into a change of analog voltage signal as labelled C.

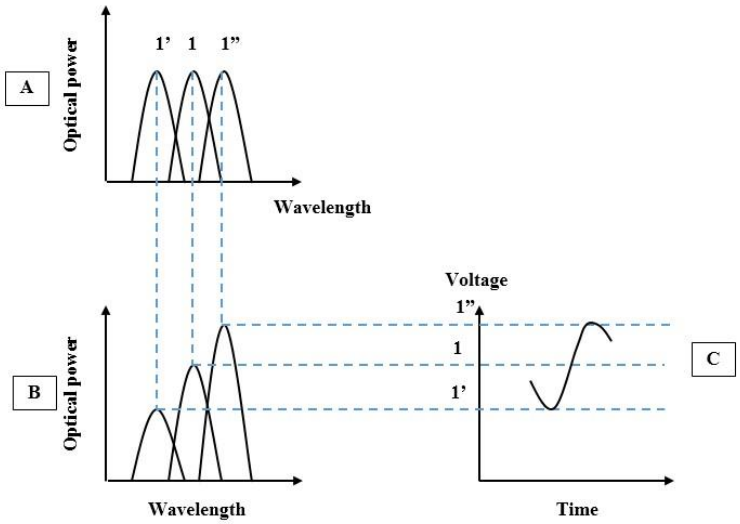

Figure 6. The working principle of photodetector [22].

3.1. Experimental procedure and results

The same experimental set-up as shown in figure 3 was maintained and adopted. Edge filter detection interrogation system configuration as shown in figure 7 was used for the experimentation.

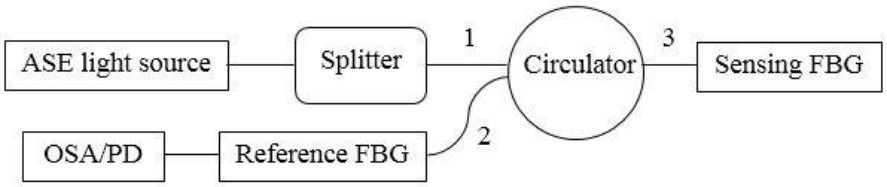

Figure 7. The configuration of edge filter detection interrogation system.

Figure 8 shows the reflected wavelength from sensing and reference FBG when both the FBGs were connected to port 3 and viewed from OSA connected to port 2. Reflected spectrum from the reference FBG is positioned to the left of the sensing FBG prior to measurement. It is also observed that the sensing FBG has slightly higher intensity than the reference FBG of about 3.76%. The reference FBG was then connected to port 2 and sensing FBG remained at port 3, figure 9 shows the recorded reflected wavelength and intensity from the mismatched between sensing and reference FBG when no load exerted.

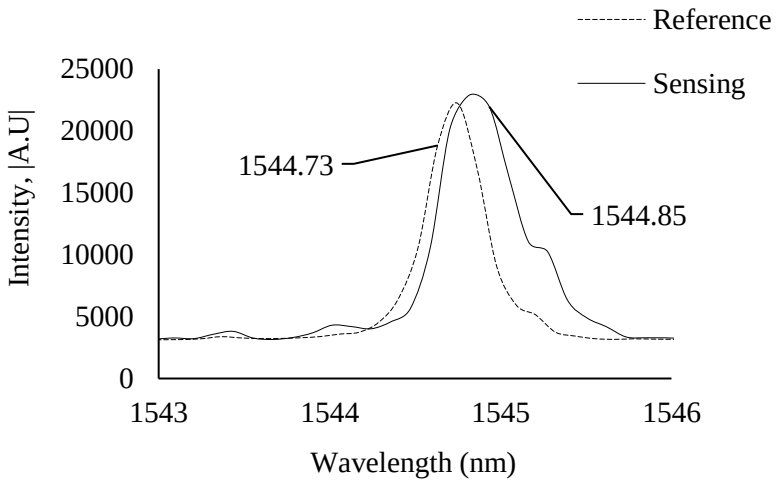

Figure 8. Reflected wavelength spectrum from sensing and reference FBG.

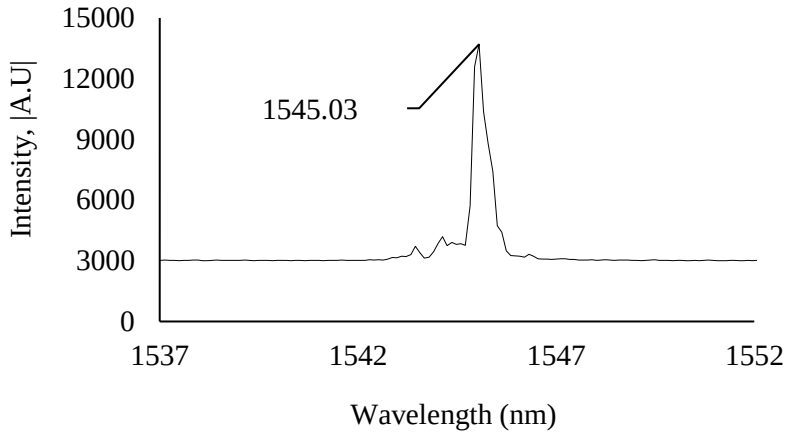

Figure 9. Reflected wavelength and intensity from the mismatched between sensing and reference FBG.

As load from 0 N to 50 N started to induce on the specimen, the reflected mismatched wavelength started to shift to the right with a constant and linear pattern. For a clear viewing in the shifting of reflected mismatched peak wavelength and increase of intensity amplitude, figure 10 shows the simplified Gaussian Bragg wavelength shift with an offset of 0.1 nm/N. The spectrum shift shows that when the load was induced from 0 N to 50 N, the peak wavelength shift from initial of 1545.03 nm to 1545.07 nm and an increasing intensity waveform was recorded. The maximum intensity recorded at 50 N of the load which is 17068 while the minimum intensity was at 0 N which is 13880.40, as expected.

Lastly, the intensity shift was converted to voltage readings with the replacement of OSA with PD. Five repetitions of voltage response against applied load were recorded and calibration to convert the voltage response to load induced were carried out. Initially, the calibration was formulated by averaging the linearity curves and without the voltage normalization algorithm as in figure 11. MATLAB real-time GUI with the substitution of linearity equation obtained was used to record the voltage response variation as the plate was induced with load as shown in figure 12. The data points correlate to the recorded voltage variations and the solid line is the line of best fit where the sensitivity is 2.4 mV/N. The dashed line is the expected voltage due to applied load calculated from the linearity equation.

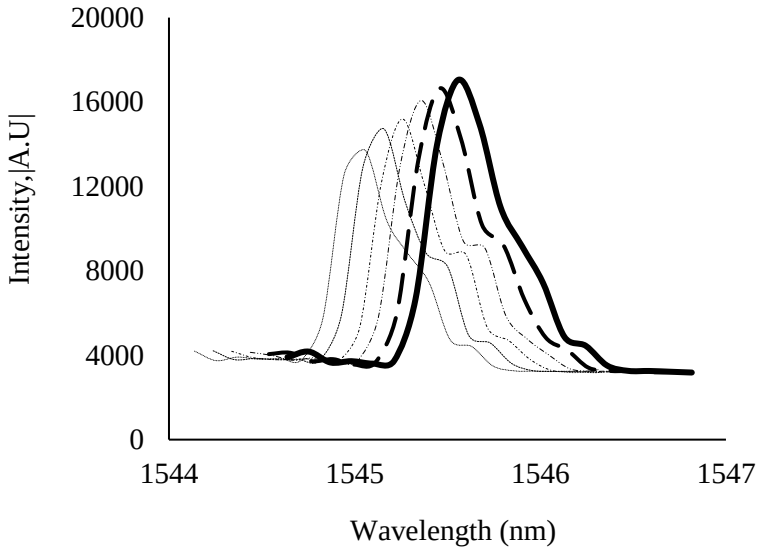

Figure 10. Reflected mismatched Bragg wavelength and intensity shift from 0 N to 50 N. The increase in line's weight correlate to the increase in loadings.

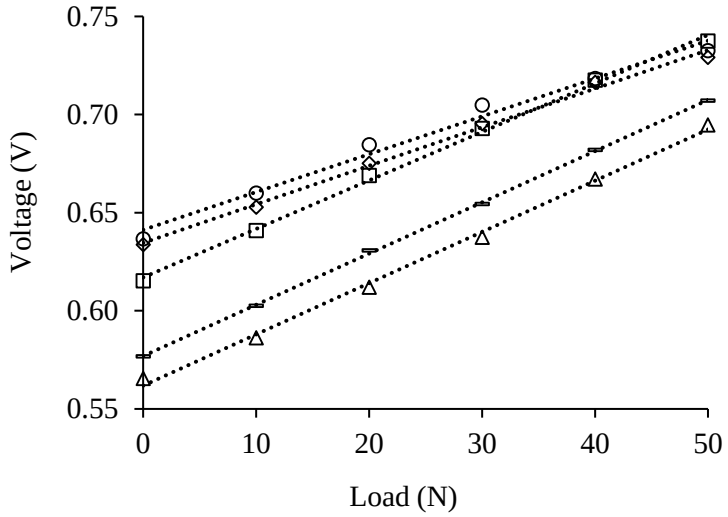

Figure 11. The linearity curves of voltage response against applied load without normalization.

Next, with the same voltage response the calibration was formulated by averaging the linearity curves and ratio scale voltage normalization algorithm was implemented as shown in figure 13. The ratio voltage normalization, $\boldsymbol{V_{norm}}$ can be expressed as in Equation 5.

$$\boldsymbol{V_{norm}} = \frac{\boldsymbol{V_s}}{\boldsymbol{V_r}} \tag{5}$$

where $\boldsymbol{V_s}$ is the voltage reading from the FBG sensor subjected to strain. Reference voltage, $\boldsymbol{V_r}$ is the reference voltage which is the initial voltage from the light source. Substituting Equation 5 into averaging linearity equation obtained from figure 13 can be expressed as in Equation 6.

$$\frac{\boldsymbol{V_s}}{\boldsymbol{V_r}} = \boldsymbol{m_{avg}\chi + C_{avg}} \tag{6}$$

where $\boldsymbol{m_{avg}}$ is the average gradient of the five voltage response, $\boldsymbol{\chi}$ is the independent variable load induced and $\boldsymbol{C_{avg}}$ is the average y-intercept.

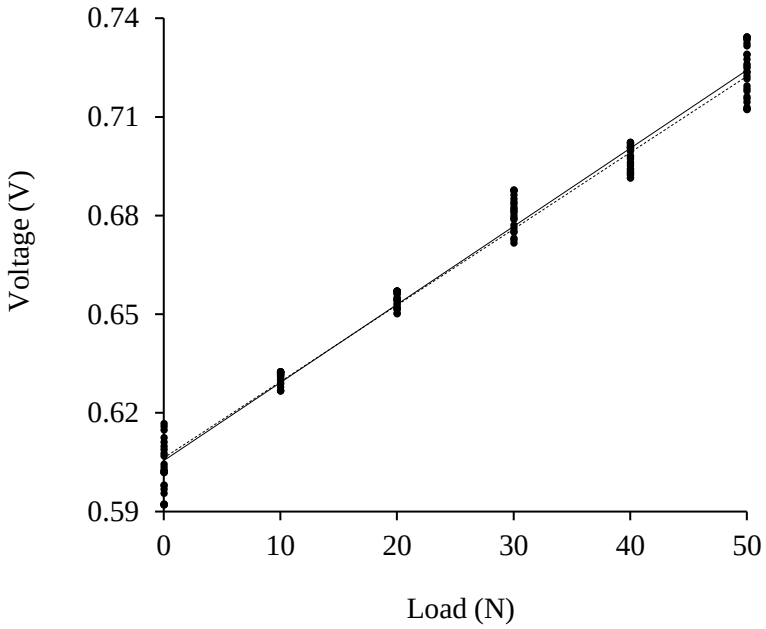

Figure 12. Output voltage variations as a function of applied load without normalization.

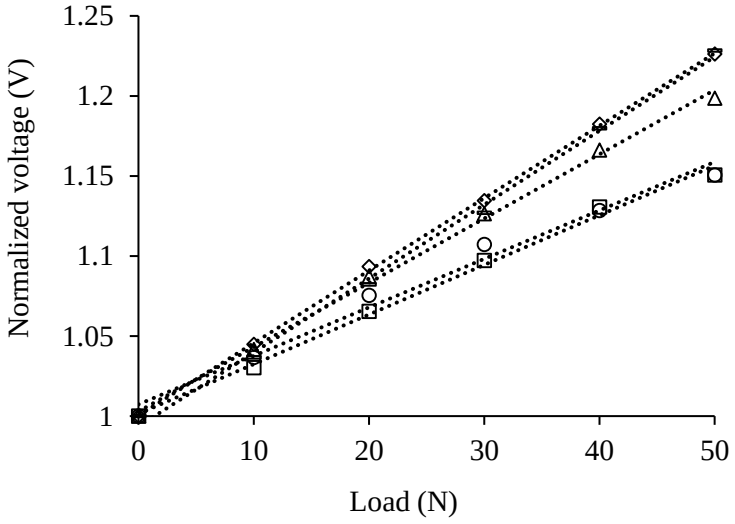

Figure 13. The linearity curves of voltage response against applied load with voltage normalization.

MATLAB real-time GUI with the substitution of voltage normalization linearity equation obtained was used to record the voltage response variation as shown in figure 14. A delay of 1 second has been programmed in the real-time GUI to reduce the data response. The data points correlate to the recorded voltage variations and the solid line is the line of best fit where the sensitivity is 3.8 mV/N. The dashed line is the expected voltage due to applied load calculated from the linearity equation. Table 1 summarizes the results of the range of load detected using non-normalization method obtained from the voltage variations in figure 12. The highest average percentage of error is 2.19% which is during 10 N load induction. The total average percentage of error is 5.35%. Table 2 summarizes the results of the range of load detected using normalization method obtained from the voltage variations

in figure 14. The highest percentage of error is 1.65% which is during 10 N load induction. The total average percentage of error is 1.38%.

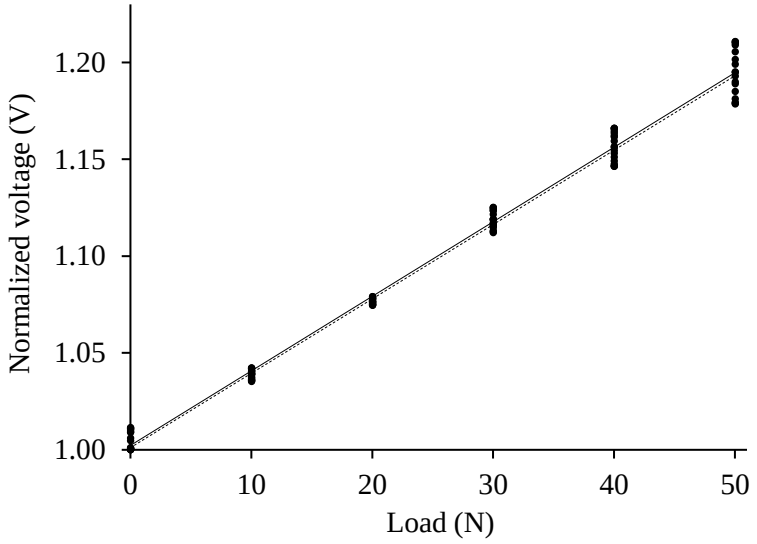

Figure 14. Output voltage variations as a function of applied load with voltage normalization.

Table 1. Range of load detected and percentage of error from the voltage variations obtained in figure 12 for non-normalization method.

Load (N)	Average load estimated (N)	Average percentage of error (%)
10	11.22	12.19
20	18.77	6.14
30	30.16	0.55
40	41.82	4.54
50	48.34	3.32
	Average percentage of error	5.35

Table 2. Range of load detected and percentage of error from the voltage variations obtained in figure 14 for normalization method.

Load (N)	Average load estimated (N)	Average percentage of error (%)
10	9.84	1.65
20	19.76	1.22
30	30.63	2.12
40	40.41	1.02
50	50.44	0.88
	Average percentage of error	1.38

4. Discussion

Optimization of optical circulator as a component in optical signal interrogation system resulted in high optical intensity. This is due to the working principle of the circulator itself in which its function is to circulate the full intensity of the light signal from the light source in one direction from port to port. In 50:50 optical coupler, the light entering as input is split into two 50% equally divided outputs. However in this experimentation, due to the high power of the ASE light source, only 10.78% of

intensity was reduced. The high power from the light source resulted in the present of unwanted wavelengths that consequence in noise and a huge range of voltage variations during mismatching with reference FBG. 1:8 splitter has the same function as an optical coupler in which the input is split into eight equally divided ratio outputs. In the experimentation, 66.4% of intensity has been reduced and an ideal reflected Bragg wavelength was achieved.

Splitter configuration has been used throughout the experimentation since it is capable of reducing the intensity and eliminate possible noise. However, a well-built real-time monitoring system with the systematic algorithm is still necessary to attain the accurate or close to exact desired values. Replacement of OSA with PD and the capitalization of edge filter interrogation system authenticate that the low-cost interrogation system eradicates the use of expensive interrogation devices and at the same demonstrate that the interrogation system adequate with any low-cost electronic data acquisition devices such as NI-DAQ or programmable logic controller (PLC). From the results of the experimentation, it is noted that when the Bragg wavelength of the sensing FBG is adjusted to the right of the filter Bragg wavelength, the PD electrical voltage output will increase as the Bragg grating elongated.

Ratio normalization of voltage response decent in organizing a cluttered and scattered data as in figure 11 to a well-organized and correlate statistical data as in figure 13. The time delay coded in MATLAB GUI has reduced the voltage data points from 26 data/minute (figure 12) to 17 data/minute (figure 14) hence restraint the range of voltage variations from redundancy. The sensitivity of the plate has increased excessively to 3.8 mV/N after normalization. Normalization method also shows great accuracy against load induced in which the total average percentage of error is only 1.38% which falls in the acceptable range of errors. Although the total average percentage of error between non-normalization method and normalization method do not have much difference. However, the greatest dominance of voltage normalization is the cut-out of pre-calibration each time before operation since the voltage normalization is expressed in the ratio of dependent voltage due to load induced over initial no load voltage readings. Non-normalization linearity curve is only accurate at once and needs to calibrate each time before use since the output voltage is varied and not consistent.

5. Conclusions

Three optical components namely optical circulator, optical coupler, and splitter have been experimentally tested and results show that splitter which has the most intensity reduction obtained an ideal reflected Bragg wavelength. The practice of low-cost edge filter interrogation system with photodetector gives an upper-hand to the low-cost interrogation system to be compatible with electronic devices. However, the utilization of photodetector to convert the intensity shift to voltage readings resulted in the inconsistency of voltage readings. Thus, the implementation of robust MATLAB GUI real-time monitoring system with voltage normalization algorithm shows that the sensitivity has increased to 3.8 mV/N and the total percentage of average error is only 1.38%. The employment of the low-cost edge filter interrogation system has eliminated the use of expensive and bulky size interrogation devices while the implement of MATLAB GUI real-time monitoring system with voltage normalization has put the FBG monitoring system into a more mature readiness level.

Acknowledgments

The authors would like to thank the Faculty of Mechanical Engineering, University Malaysia Pahang for providing laboratory facilities and financial support. They would also like to thank the Photonics Research Centre University Malaya (PRCUM), for their support in fabricating the FBGs. Finally, special thanks to the Malaysian Ministry of Higher Education for providing the FRGS grant RDU160136.

References

[1] Pereira G, Frias C, Faria H, Frazao O and Marques A T 2013 On the improvement of strain measurements with FBG sensors embedded in unidirectional composites *Polymer Testing* **32** 99-105

[2] Dai Y, Li P, Liu Y, Asundi A and Leng J 2014 Integrated real-time monitoring system for strain/temperature distribution based on simultaneous wavelength and time division multiplexing technique *Optics and Lasers in Engineering* **59** 19-24
[3] Zou H, Liang D and Zeng J 2012 Dynamic strain measurement using two wavelength matched fiber Bragg grating sensors interrogated by a cascaded long period fiber grating *Optics and Lasers in Engineering* **50** 199-203
[4] Ling H Y, Lau K T, Cheng L and Jin W 2006 Viability of using an embedded FBG sensor in a composite structure for dynamic strain measurement *Measurement* **39** 328-34
[5] Ma, Wang X, Ma Y, Zhou P and Liu Z 2014 Analysis of multi-wavelength active coherent polarization beam combining system *Optics Express* **22** 16538-51
[6] Allwood G, Wild G, Lubansky A and Hinckley S 2015 A highly sensitive fiber Bragg grating diaphragm pressure transducer *Optical Fiber Technology* **25** 25-32
[7] Ma, Zhao M, Huang X, Bae H, Chen Y and Yu M 2016 Low cost, high performance white-light fiber-optic hydrophone system with a trackable working point *Optics Express* **24** 19008-19
[8] Stephens R, Plew R and Jones A D 2008 *Sams teach yourself SQL in 24 hours*: Pearson Education)
[9] Ioffe S and Szegedy C 2015 Batch normalization: Accelerating deep network training by reducing internal covariate shift *arXiv preprint arXiv:1502.03167*
[10] Pelz C R, Molly K M, Bagby G and Sears R C 2008 Global rank invariant set normalization (GRSN) to reduce systematic distortions in microarray data *BMC bioinformatics* **9** 1-
[11] Sboner A, Karpikov A, Chen G, Smith M, Dawn M, Freeman L C, Schweitzer B and Gerstein M B 2009 Robust linear model normalization to reduce technical variability in functional protein microarrays *Journal of proteome research* **8** 5451-64
[12] Wang L and Wei Y 2016 Revised normalized difference nitrogen index (NDNI) for estimating canopy nitrogen concentration in wetlands *Optik - International Journal for Light and Electron Optics* **127** 7676-88
[13] Fusiek G, Orr P and Niewczas P Temperature-independent high-speed distributed voltage measurement using intensiometric FBG interrogation. In: *2015 IEEE International Instrumentation and Measurement Technology Conference (I2MTC) Proceedings,* pp 1430-3
[14] Kanellos G T, Papaioannou G, Tsiokos D, Mitrogiannis C, Nianios G and Pleros N 2010 Two dimensional polymer-embedded quasi-distributed FBG pressure sensor for biomedical applications *Optics Express* **18** 179-86
[15] Kashyap R 1999 *Fiber bragg gratings*: Academic press)
[16] Park J M, Lee S I, Kwon O Y, Choi H S and Lee J H 2003 Comparison of nondestructive microfailure evaluation of fiber-optic Bragg grating and acoustic emission piezoelectric sensors using fragmentation test *Composites Part A: Applied Science and Manufacturing* **34** 203-16
[17] Majumder M, Gangopadhyay T K, Chakraborty A K, Dasgupta K and Bhattacharya D K 2008 Fibre Bragg gratings in structural health monitoring - Present status and applications *Sensors and Actuators A: Physical* **147** 150-64
[18] Wild G and Hinckley S 2010 Optical fibre Bragg gratings for acoustic sensors. In: *Proc. 20th International Congress on Acoustics,* pp 23-7
[19] Lee, Jeong Y, Yin S, Ruffin P B and Yu F T S 2008 Interrogation techniques for fiber grating sensors and the theory of fiber gratings *Fiber Optic Sensors. Taylor & Francis* 253-331
[20] Webb D J, Surowiec J, Sweeney M, Jackson D A, Gavrilov L R, Hand J W, Zhang L and Bennion I 1996 Miniature fiber optic ultrasonic probe. In: *SPIE's 1996 International Symposium on Optical Science, Engineering, and Instrumentation,* pp 76-80
[21] Tsuda H 2005 Ultrasound and damage detection in CFRP using fiber Bragg grating sensors *Composites Science and Technology* **66** 676-83
[22] Hafizi Z M 2014 The applications of near infra-red fibre Bragg grating sensors for wave propagation based structural health monitoring of thin laminated composite plates.